JBIC Journal of Biological Inorganic Chemistry (2019) 24:899–908
https://doi.org/10.1007/s00775-019-01707-9

ORIGINAL PAPER

Monofunctional platinum(II) compounds and nucleolar stress: is phenanthriplatin unique?

Christine E. McDevitt[1] · Matthew V. Yglesias[1,2] · Austin M. Mroz[1,3] · Emily C. Sutton[2,4] · Min Chieh Yang[1,3] · Christopher H. Hendon[1,3] · Victoria J. DeRose[1,2,3]

Received: 17 July 2019 / Accepted: 13 August 2019 / Published online: 7 September 2019

Abstract

Platinum anticancer therapeutics are widely used in a variety of chemotherapy regimens. Recent work has revealed that the cytotoxicity of oxaliplatin and phenanthriplatin is through induction of ribosome biogenesis stress pathways, differentiating them from cisplatin and other compounds that mainly work through DNA damage response mechanisms. To probe the structure–activity relationships in phenanthriplatin's ability to cause nucleolar stress, a series of monofunctional platinum(II) compounds differing in ring number, size and orientation was tested by nucleophosmin (NPM1) relocalization assays using A549 cells. Phenanthriplatin was found to be unique among these compounds in inducing NPM1 relocalization. To decipher underlying reasons, computational predictions of steric bulk, platinum(II) compound surface length and hydrophobicity were performed for all compounds. Of the monofunctional platinum(II) compounds tested, phenanthriplatin has the highest calculated hydrophobicity and volume but does not exhibit the largest distance from platinum(II) to the surface. Thus, spatial orientation and/or hydrophobicity caused by the presence of a third aromatic ring may be significant factors in the ability of phenanthriplatin to cause nucleolar stress.

Graphic abstract

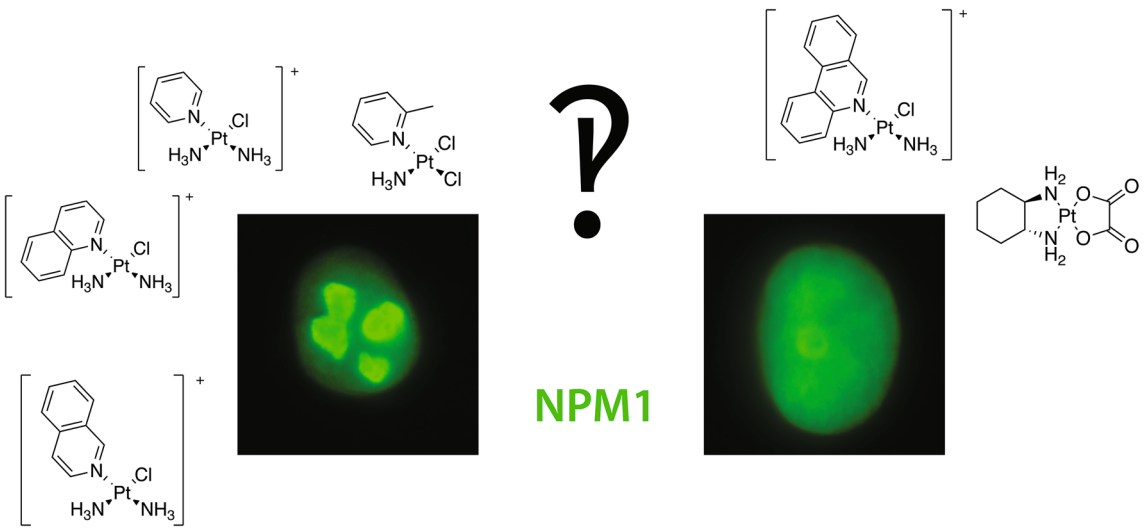

Keywords Platinum · Anticancer drug · Cell death · Structure–activity relationship · Computational chemistry · Imaging · Nucleolus

✉ Victoria J. DeRose
derose@uoregon.edu

Extended author information available on the last page of the article

Introduction

Platinum-based drugs are an important class of chemotherapeutics. After the initial discovery of the anti-proliferative capabilities of cisplatin, the drug was FDA approved in 1978 and continues to be in significant use over 40 years later [1]. Two additional Pt(II) compounds were subsequently approved by the FDA, carboplatin in 1989 and oxaliplatin in 1996. Improvements upon these three drugs have been attempted and some new compounds even entered into clinical trials, but none have been approved by the FDA [2].

The three FDA-approved drugs are all considered classical platinum compounds. The characteristics of classical compounds are a result of early structure–activity relationship (SAR) studies that determined the necessary properties for platinum compounds to exhibit anti-proliferation activity [3]. These required components are that the platinum compound be square planar, have a neutral overall charge, and contain two non-labile *cis*-am(m)ines and two labile *cis* anionic ligands. Although these rules led to the drugs that are used today, research into compounds that would not be within a traditional SAR study have produced non-classical platinum drugs with anti-proliferative activity. These non-classical compounds include Pt(IV) prodrugs, monofunctional, trans-platinum, polyplatinum, and tethered platinum complexes [3, 4]. One of the most effective and well-studied non-classical compounds is the monofunctional Pt(II) phenanthriplatin [3, 5] (Fig. 1). In addition to having only a single exchangeable anionic ligand, the *N*-heterocyclic ligand of phenanthriplatin and others of this class, such as pyriplatin (Fig. 1), is rotated perpendicular to the square-planar Pt ligand plane.

Phenanthriplatin has exhibited unique activity in the NCI-60 cell line screen when compared to other platinum chemotherapeutics [5]. Phenanthriplatin is significantly more potent with a 7–40× higher toxicity than cisplatin [3, 5]. It has higher cellular uptake than cisplatin or pyriplatin [5]. In addition, the phenanthridine ligand of phenanthriplatin may facilitate rapid DNA binding through reversible intercalation between nucleobases before platinum binding occurs [6]. Studies have also revealed some of the biological targets of phenanthriplatin. It has been shown to act as a topoisomerase II poison [7]. Phenanthriplatin also was demonstrated to inhibit RNA polymerase II [8], but allows efficient DNA polymerase η bypass [9]. Overall, these studies have shown that phenanthriplatin can affect biological processes in a variety of ways, and this has led researchers to suggest that the effectiveness of the compound is through multiple cellular pathways [10].

In a recent study, the classical platinum compound oxaliplatin and non-classical phenanthriplatin were both shown to induce ribosome biogenesis stress as the primary pathway to cell death [11]. This surprising observation is in contrast with cisplatin and carboplatin, which were shown to cause

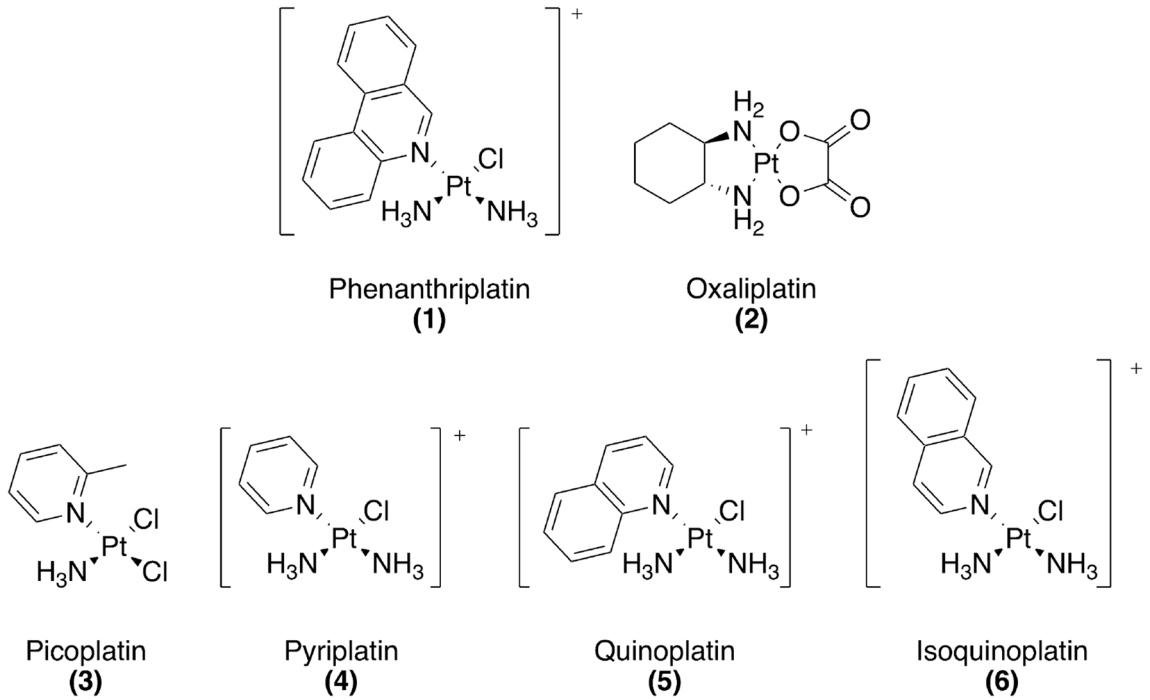

Fig. 1 Platinum compounds used in this study

cell death through DNA damage as is expected for classical compounds. The ability to induce nucleolar stress shared between oxaliplatin and phenanthriplatin is perplexing considering the major structural differences between the two compounds. We endeavored to determine whether there were structural similarities between these two molecules which would explain this similar activity, and determine whether the ability to induce nucleolar stress was inherent to the family of non-classical monofunctional platinum(II) compounds. To do this, we synthesized a suite of monofunctional and related platinum compounds (Fig. 1) and analyzed their ability to cause nucleolar stress by measuring nucleophosmin (NPM1) relocalization. We further compared structural and electronic properties of these compounds based on DFT calculations. We find that phenanthriplatin, but not related quinoplatin or isoquinoplatin, induces nucleolar stress as measured by NPM1 relocalization in human lung carcinoma A549 cells. Although phenanthriplatin has the largest total volume and hydrophobicity of the compounds tested, quinoplatin and isoquinoplatin may have similar potential to disrupt intermolecular interactions based on Pt-ligand distances. We conclude that the unique ability of phenanthriplatin to induce nucleolar stress is conferred by the third aromatic ring. The ligand disposition of these monofunctional *N*-heterocyclic Pt(II) compounds is sufficiently different from oxaliplatin to suggest that separate properties of oxaliplatin and phenanthriplatin lead to their abilities to both cause nucleolar stress.

Materials and methods

Reagents and synthesis

Cisplatin [12], picoplatin [13], and pyriplatin, quinoplatin, isoquinoplatin, and phenanthriplatin [5] were synthesized as previously reported. Oxaliplatin was purchased from TCI America. Actinomycin D was purchased from Thermo Fisher Scientific. A549 cell line was acquired from the American Type Culture Collection.

Cell culture and treatment

A549 human lung carcinoma cells (#CCL-185, American Type Culture Collection) were cultured at 37 °C, 5% CO_2 in DMEM supplemented with 10% FBS and 1% antibiotic–antimycotic. A549 cells have been used previously to study nucleolar stress pathways [14, 15]. Cells between passage 11–25 and at confluency of 70% were used in the treatments. Cells were treated for 24 h with 10 μM compound, with the exception of phenanthriplatin and phenanthridine which were administered at 0.5 μM and actinomycin D at 5 nM. The counterion for positively-charged compounds is nitrate. Stock solutions of 5 mM compound in DMF were made and used with the exception of oxaliplatin, which was made in water and actinomycin D which was made in DMSO. Immediately prior to treatment, platinum compounds were diluted into media. Final DMF and DMSO concentrations were 0.2% (v/v) in media. We chose to use 0.5 μM phenanthriplatin to account for the higher cellular accumulation of phenanthriplatin and to be more in line with reported 72 h IC_{50} values which are not exhibited by the other studied compounds [5].

Immunofluorescence

Cells to be imaged were grown on coverslips (Ted Pella product no 260368, Round glass coverslips, 10-mm diam, 0.16–0.19-mm thick) as described above. Following treatment, cells were washed twice with PBS. They were then fixed for 20 min at room temperature in 4% paraformaldehyde diluted in PBS. Cells were permeabilized with 0.5% Triton-X in PBS for 20 min at room temperature followed by two 10-min blocking steps with 1% BSA in PBST. The cells were incubated for 2 h using primary antibody (NPM1 Monoclonal Antibody, FC-61991, from Thermo Fisher, 1:200 dilution in PBST with 1% BSA) and 1 h in secondary antibody (Goat Anti-Mouse IgG H&L Alexa Fluor® 488, ab150113, Abcam, 1:1000 dilution in PBST with 1% BSA). Between each incubation and before mounting, slides were washed three times for 5 min each using PBST. Coverslips were mounted on slides with ProLong™ Diamond Antifade Mountant with DAPI (Thermo Fisher) according to manufacturer's instructions.

Imaging and quantification

Images were taken using a HC PL Fluotar 63×/1.3 oil objective mounted on a Leica DMi8 fluorescence microscope with Leica Application Suite X software. Quantification of NPM1 relocalization was performed in an automated fashion using a Python 3 script. Images were preprocessed in ImageJ [16, 17] to convert the DAPI and NPM1 channels into separate 16-bit greyscale images. Between 100 and 250 cells were analyzed for each treatment group. Nuclei segmentation was determined with the DAPI images using Li thresholding functions in the Scikit-Image Python package [18]. The coefficient of variation (CV) for individual nuclei, defined as the standard deviation in pixel intensity divided by the mean pixel intensity, was calculated from the NPM1 images using the SciPy Python package. All data were normalized to the no-treatment control in each experiment. NPM1 imaging results for each compound were observed on two separate testing days. Duplicates of treatments were performed and analyzed and are available upon request from the corresponding author.

Computations

Based on the experimental results, we hypothesized that the size, shape or hydrophobicity of the platinum(II) compounds may be instructive in correlating the biological activity with the chemical structure because of biological implications of these structural components in an interaction between two biomolecules that may be disrupted. Thus, we optimized all platinum(II) compounds using density functional theory (DFT) as implemented in Gaussian09 [19] so that we might quantitatively assess the structural differences and hydrophobicity of the compounds.

Geometry optimizations were performed with an RMS force convergence criterion of 10^{-5} hartree. The electronic wavefunction was minimized using the GGA functional PBE [20, 21], with the DEF2TZP basis set. Relativistic effects were not explicitly included, however, these were not expected to significantly impact the geometries of the platinum(II) complexes [22]. Solvent was implicitly included using the Solvent Model Density method [23].

The solvent-dependent difference in Gibbs free energies ($\Delta G_{\text{water–octanol}}$) was calculated using

$$\Delta G_{\text{water–octanol}} = \Delta G_{\text{water}} - \Delta G_{\text{octanol}},$$

where (ΔG_{water}) and ($\Delta G_{\text{octanol}}$) are the change in free energies of the system in water and *n*-octanol, respectively. (ΔG_{water}) was computed using the structure optimized in the pseudo solvent, water. This optimized structure was kept constant for all subsequent computations, including calculation of the compound in pseudo-solvent, *n*-octanol, which yielded ($\Delta G_{\text{octanol}}$). This approach minimizes the reorganizational energetic differences. Thus, ($\Delta G_{\text{water–octanol}}$) is a measure of the hydrophobicity for each compound.

Further calculations were required to assess the size and shape of the platinum(II) compounds. Two measures of size were considered, (i) volume, and (ii) the longest vector between the platinum atom and the surface of the molecule. The latter characteristic represents the main steric component of the ligand in each compound.

To quantitatively assess the volume of each compound, a definition of size is necessary. Thus, we will use the presence of electron density to signify the location of the chemical system. Since DFT yields both the electron density and electrostatic potential of the optimized, non-hydrolyzed platinum(II) compound structures and we have previously developed a tool to analyze the electrostatic potential of chemical systems [24], we will use the same file format to analyze the electrostatic potential. As a result, the electrostatic potentials of the optimized structures were computed by minimizing the electronic wavefunction using a 500 eV planewave cutoff, a gamma-only k-grid, and the PBE [20, 21] functional utilizing a plane-augmented wave (PAW) [25, 26] basis as implemented in the Vienna Ab initio Software Package (VASP) [27–30]. All compounds were calculated within a sufficiently large computational box to minimize self-interaction.

The electric field is the gradient of the electrostatic potential; thus, the electric field embodies the direction of greatest increase in electrostatic potential. This is significant because the increased slope of the electric field enables us to more clearly define the edge of a chemical system in space. Therefore, deriving the electric field from the electrostatic potential returned by DFT allows us to assess the size of each compound by sampling the electric field. However, to achieve this, definition of a surface needs to be addressed.

We will define the edge of a chemical system as the point where the electric field magnitude no longer changes, which is intuitive considering the definition of the electrostatic potential. Since DFT calculations return electrostatic potential values on the order of 10^{-6} eV, a change in less than 10^{-5} eV is considered negligible. This approach is based on previous atomic radii calculations, which employ negligible change in electron density to assess the size of atoms [25, 26].

Using the area of each compound defined by sampling the electric field, the longest vector between the platinum atom and the surface was calculated for each compound, capturing the main steric component of each ligand.

Results and discussion

Oxaliplatin and phenanthriplatin cause NPM1 relocalization

A previous study examining cell death mechanisms of phenanthriplatin **(1)** and oxaliplatin **(2)** has shown that both compounds cause cell death through ribosome biogenesis stress [11]. For the current studies, we monitored NPM1 relocalization from the nucleolus to the nucleoplasm, which is a hallmark of nucleolar stress resulting from the disruption of ribosome biogenesis [31]. Under non-stressed conditions, NPM1 is localized to the nucleolus; however, NPM1 is distributed throughout the nucleoplasm following nucleolar stress. We set out to measure the extent of NPM1 relocalization when cells were treated with a series of platinum compounds with cyclic ligands and either monofunctional or bifunctional substitution properties.

We first examined NPM1 relocalization following treatment with oxaliplatin and phenanthriplatin. As expected, known ribosome biogenesis stress inducer actinomycin D caused NPM1 relocalization to the nucleoplasm while the negative no-treatment control showed NPM1 localized in the nucleoli (Fig. 2a). Both oxaliplatin and phenanthriplatin caused relocalization of NPM1 throughout the nucleus,

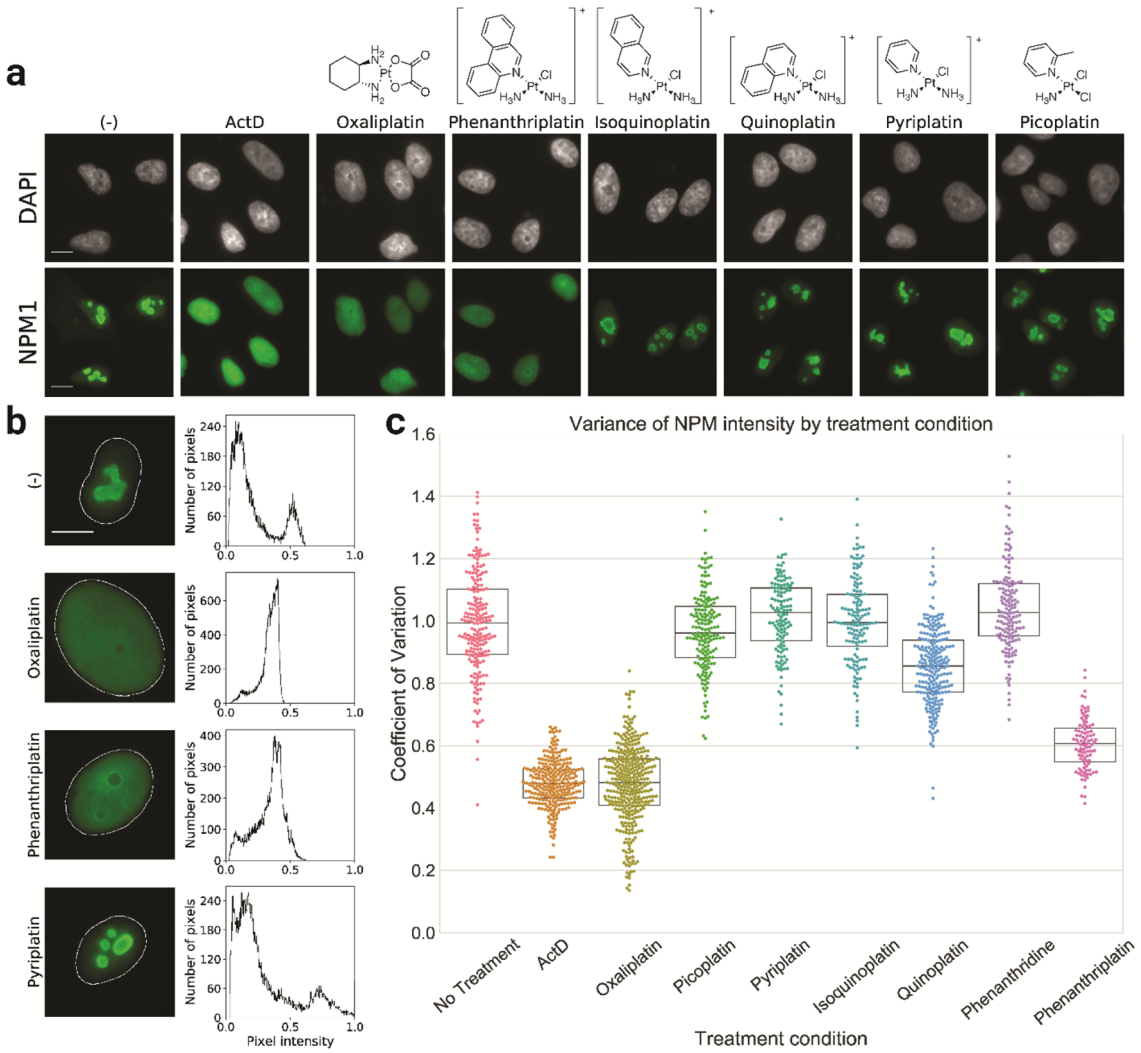

Fig. 2 NPM1 relocalization. **a** Representative images for each platinum treatment. DAPI (grey) shows the nucleus of A549 cells. NPM1 (green) is evenly distributed in positive control actinomycin D (ActD), and also in cells treated with oxaliplatin, and phenanthriplatin, indicating nucleolar stress. NPM1 is localized to the nucleolus in untreated cells, and cells treated with isoquinoplatin, quinoplatin, pyriplatin, and picoplatin. Scale bar is 10 μm. Cells were treated with 10 μM platinum at 24 h with the exception of phenanthriplatin and phenanthridine which were used at 0.5 μM. **b** Representative histograms for individual cells. In untreated negative control and pyriplatin-treated cells, large populations of pixels are found at low and high intensity. NPM1 localization throughout the nucleoplasm is seen following oxaliplatin and phenanthriplatin treatment with pixel intensity centered around 0.4. **c** Coefficient of variation for platinum treatments. CV values for individual nuclei are plotted for each treatment group. Box plot center line represents the median, and the bottom and top limits represent the first and third quartile, respectively. The CV from each cell is normalized to the mean CV from the no-treatment control sample. Populations that have NPM1 relocalized have a median CV of around 0.6 while populations without NPM1 relocalization are around 1

confirming their ability to cause nucleolar stress as previously reported [11].

To determine the extent of nucleolar stress, we quantified the heterogeneity of nuclear NPM1 intensity distribution by its coefficient of variation (CV). The CV is the standard deviation of the pixel intensity populations corresponding to NPM1-based immunofluorescence normalized by the mean intensity of each nucleus. In cells that are undergoing nucleolar stress, NPM1 is relatively evenly diffused throughout the nucleus, leading to homogeneous intensities and a small CV. Histograms of representative cells show a large population of medium intensity pixels across the cell for compounds that cause NPM1 relocalization (Fig. 2b). For cells that are not undergoing stress, NPM1 is concentrated in the periphery of the nucleolus while being absent in the nucleoplasm, resulting in a heterogeneous population of pixel intensities and a high CV. Histograms of cell images from compounds that do not cause NPM1 relocalization show large populations at the two extremes of the pixel intensity which would result in a large CV (Fig. 2b).

CVs were calculated for each cell in a population and the distribution of these CVs was evaluated for each treatment condition. Corresponding to our representative NPM1 images (Fig. 1a), compounds that caused no NPM1 redistribution had median CVs around 1 (when normalized to the no-treatment control) while compounds that caused NPM1 relocalization had medians at or lower than 0.6 (normalized to the no-treatment control). NPM1 relocalization was observed upon treatment with oxaliplatin, phenanthriplatin and actinomycin D (Fig. 2c). Additionally, treatment with the phenanthridine ligand alone is not sufficient to induce nucleolar stress (Fig. 2c).

Picoplatin does not cause NPM1 relocalization

There are large structural differences between oxaliplatin and phenanthriplatin; however, these disparate compounds are both able to activate nucleolar stress pathways whereas cisplatin does not. Both the DACH ligand of oxaliplatin and the phenanthridine ligand of phenanthriplatin add significant steric bulk in comparison with cisplatin. However, phenanthriplatin is a monofunctional compound. In addition, unlike the case of oxaliplatin, in phenanthriplatin, the phenanthridine rings are oriented perpendicular to the square-planar Pt ligand plane [5]. Picoplatin **(3)** is one compound that bridges these differences in that the picoline ring is oriented perpendicular to the platinum plane [32]. Picoplatin is also a classical bifunctional platinum compound and enabled us to determine whether the added ligand bulk regardless of orientation was sufficient to induce NPM1 relocalization. In A549 cells treated with picoplatin, NPM1 did not relocalize to the nucleoplasm (Fig. 2a) as quantified by a median CV of around 1 (Fig. 2c), indicating that picoplatin does not cause nucleolar stress.

NPM1 relocalization is not a general property of monofunctional platinum compounds

After determining that the classical compound picoplatin did not cause NPM1 relocalization despite having some similarities to oxaliplatin in terms of added ring and steric bulk, we next examined the properties of non-classical monofunctional platinum compounds. We synthesized three additional monofunctional compounds that have one or two aromatic rings to test whether nucleolar stress was inherent to ring-containing monofunctional platinum(II) compounds as a whole or whether it was a phenomenon only exhibited by phenanthriplatin.

We had tested picoplatin and determined that the perpendicular orientation of the picoline ligand is not sufficient to cause NPM1 relocalization. To further explore the influence of ligand orientation and the binding mode of platinum, we next tested pyriplatin **(4)**. Similar to picoplatin, pyriplatin contains a single aromatic ring. However, unlike picoplatin, pyriplatin has more possible orientations of the aromatic ring due to lack of steric interference involving the methyl of the picoline [33]. In addition, pyriplatin is more similar to phenanthriplatin in being a monofunctional compound with an overall positive charge. Following a 24 h treatment at 10 μM, pyriplatin did not cause NPM1 relocalization and samples had a median CV of around 1 (Fig. 2). From this, we concluded that the ability to cause NPM1 relocalization was not inherent to the class of monofunctional platinum(II) compounds containing *N*-heterocyclic ligands.

We next considered whether steric bulk was a factor in NPM1 relocalization by examining the influence of the addition of a second ring. We synthesized the structural isomers quinoplatin **(5)** and isoquinoplatin **(6)** (Fig. 3), to test whether a second aromatic ring would be sufficient to

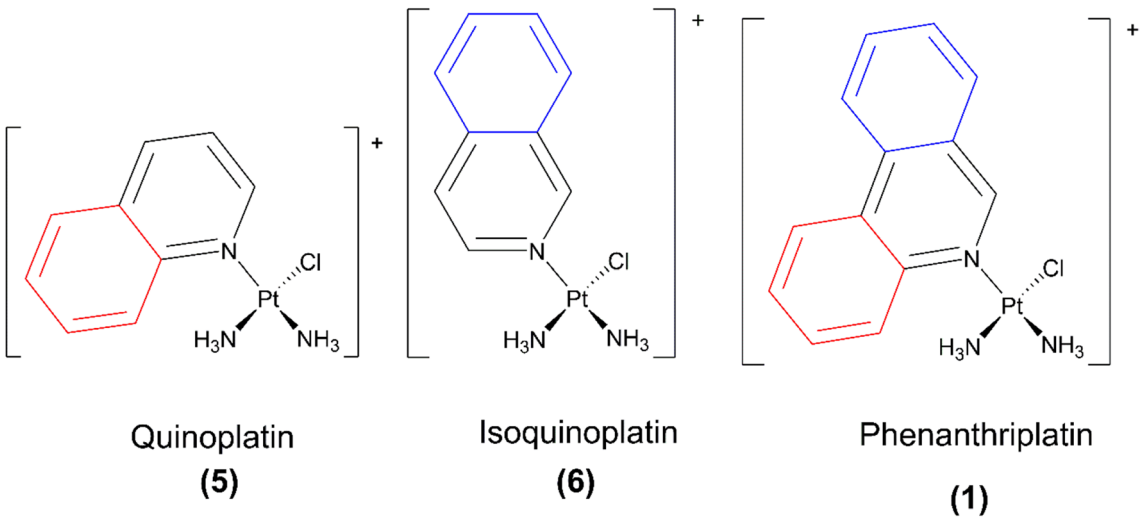

Fig. 3 Two-ring structural isomers related to phenanthriplatin

cause NPM1 relocalization. We tested these compounds and determined that neither quinoplatin nor isoquinoplatin caused increased NPM1 relocalization, with NPM1 intensities from cells treated with both compounds having a median CV of around 1 (Fig. 2). From this we concluded that for monofunctional Pt(II) compounds, the steric bulk from a second ring alone does not induce NPM1 relocalization regardless of ring orientation. This added further evidence that NPM1 relocalization was not an inherent property of this non-classical class of platinum compounds and was unique to phenanthriplatin under these conditions.

Steric bulk is not sufficient to predict NPM1 relocalization

From our data, we have determined that phenanthriplatin and oxaliplatin are unique to our suite of compounds. We next examined whether there are any trends present in steric bulk that could explain whether compounds caused NPM1 relocalization. All platinum(II) compounds were optimized using DFT (Fig. 4) and two variables were calculated to assess steric bulk. First, the volume of the optimized, non-hydrolyzed structure is obtained by sampling the respective electrostatic potential (Table 1). Oxaliplatin and phenanthriplatin were the compounds with the largest volume; however, this included the aquation-labile ligands which accounts for a large portion of oxaliplatin's volume.

Second, the magnitude of the maximum vector between platinum and the surface of the compound, where the surface of the compound is defined as the extent to which the electrostatic potential permeates in space (Table 1), was calculated. No trend was found with these distance measurements. Oxaliplatin, which caused NPM1 relocalization, had a similar maximum distance as that of quinoplatin, which did not cause NPM1 relocalization. Additionally, phenanthriplatin, which caused NPM1 relocalization had a similar distance to that of isoquinoplatin which did not cause NPM1 relocalization (Table 1). Thus, while phenanthriplatin exhibits the largest steric bulk, it does not have the maximum steric reach from platinum to the surface of the compound.

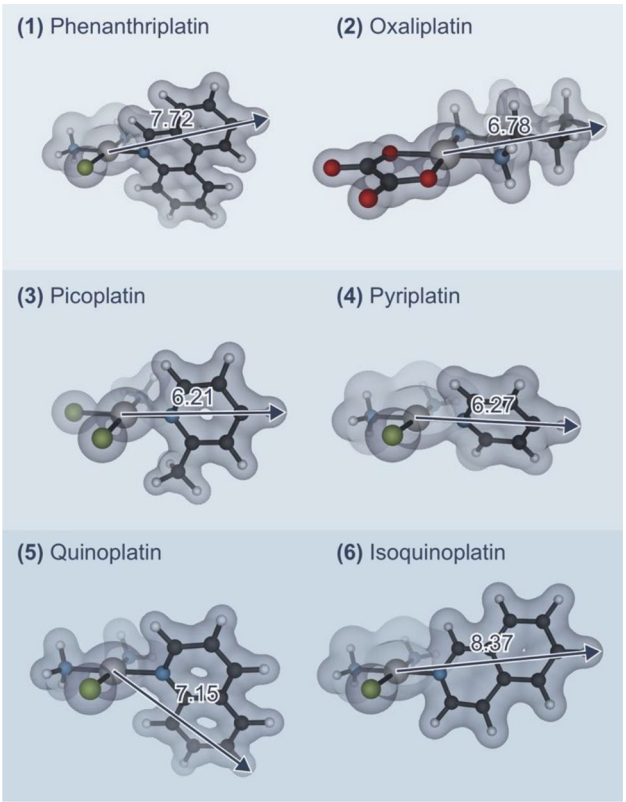

Fig. 4 Optimized structures of the platinum(II) compounds are displayed at an isosurface level of 0.25 e/Å^{-3} for each compound, as implemented in VESTA. This illustrates the volume of the molecule that is reported. The distances between the platinum atom and the surface of each compound are shown with the corresponding vector. All measurements are reported in angstrom (Å)

Hydrophobicity is not sufficient for predicting NPM1 relocalization

Hydrophobicity of the non-labile ligand may be an important factor in interrupting biomolecular interactions, or in partitioning into cellular compartments or regions of the nucleolus. We examined if there was a trend in hydrophobicity that would explain why oxaliplatin and phenanthriplatin caused NPM1 relocalization while all other compounds in our library did not. We used our optimized structures to calculate $\Delta G_{\text{water–octanol}}$ (Table 2). As expected, compounds with more aromatic rings were more hydrophobic and had more positive differences in $\Delta G_{\text{water–octanol}}$, while compounds with less rings showed the opposite trend. Phenanthriplatin is more hydrophobic than all other compounds except picoplatin, which does not cause NPM1 relocalization and is the most hydrophobic compound tested with a Gibbs solvation energy of 2.54 kcal/mol. Overall, this measure of hydrophobicity was not able to produce a trend that provides a satisfactory explanation for why oxaliplatin and phenanthriplatin

Table 1 Steric bulk measurements for platinum compounds in order of increasing volume

Compound	Volume (Å^3)	Maximum Pt-to-surface distance (Å)
Pyriplatin **(4)**	24.91	6.27
Picoplatin **(3)**	27.69	6.21
Isoquinoplatin **(6)**	31.21	8.37
Quinoplatin **(5)**	33.89	7.15
Oxaliplatin **(2)**	34.13	6.78
Phenanthriplatin **(1)**	37.25	7.72

Table 2 Gibbs free energy of transfer between octanol and water

Compound	$\Delta G_{water-octanol}$ (Kcal/mol)
Oxaliplatin **(2)**	−4.92
Pyriplatin **(4)**	−1.92
Isoquinoplatin **(6)**	−0.607
Quinoplatin **(5)**	−0.34
Phenanthriplatin **(1)**	0.94
Picoplatin **(3)**	2.54

cause NPM1 relocalization while others did not. Therefore, we conclude that hydrophobicity alone is not sufficient for causing NPM1 relocalization.

Conclusions

This work aimed to find a structural relationship between oxaliplatin and phenanthriplatin which would provide information on necessary and sufficient structural components required for these platinum compounds to induce cell death via nucleolar stress. In comparison with cisplatin, which does not cause nucleolar stress, oxaliplatin and phenanthriplatin both have significantly larger ring-containing ligands. Phenanthriplatin is also a monofunctional Pt(II) compound. To explore this question, we synthesized a library of ring-containing platinum compounds, most being monofunctional Pt(II) compounds. This library was tested for the ability to induce nucleolar stress by monitoring NPM1 relocalization, and quantifying the resulting images. First, we tested oxaliplatin and phenanthriplatin to confirm that they caused NPM1 relocalization in agreement with previous literature proposing that they cause nucleolar stress [11]. We then tested whether a heterocyclic ligand oriented perpendicular to the square-planar platinum(II) ligand plane would be sufficient by testing picoplatin, and found that picoplatin did not cause nucleolar stress as measured by NPM1 relocalization. Thus, for bifunctional platinum compounds, a ligand ring is insufficient to cause nucleolar stress.

We investigated the importance of ligand ring number and distribution in other compounds of the monofunctional platinum(II) class by testing pyriplatin, quinoplatin and isoquinoplatin. None of these compounds caused NPM1 relocalization, indicating that phenanthriplatin was unique in this class of monofunctional compounds. We note that this limited study has been performed at a single concentration and treatment time for all compounds. It is possible that longer treatment time or higher concentrations might lead to different effects, and this is being explored in further studies. None of the non-phenanthriplatin compounds cause significant levels nucleolar stress at relatively high (10 μM) treatment concentrations compared to phenanthriplatin (0.5 μM), indicating that they are in a different class than phenanthriplatin in terms of activities.

We performed DFT calculations to optimize structures and calculate the solvent-dependent difference in Gibbs free energy between water and *n*-octanol, a measure of hydrophobicity. To further investigate structural characteristics, we calculated the maximum distance from the platinum atom to the surface of each structure and volume from the DFT-optimized structures. We found no correlation between this distance and the ability to cause NPM1 relocalization. Further, there was no strong correlation between the solvent-dependent difference in Gibbs free energy between water and octanol for compounds that were able to induce NPM1 relocalization.

In view of these results, we suggest that phenanthriplatin is a unique compound in the monofunctional platinum(II) compound class in its ability to cause NPM1 relocalization. We suggest that the addition of a third aromatic ring in phenanthriplatin may play a large role in differentiating phenanthriplatin from other monofunctional platinum(II) compounds we tested for inducing nucleolar stress. The presence of a third aromatic ring increases steric bulk both above and below the square-planar platinum ligand plane. Additionally, a third ring increases hydrophobicity and provides intercalation potential to phenanthriplatin [6] in comparison to quinoplatin and isoquinoplatin. Phenanthriplatin exhibited the largest volume and was the most hydrophobic compound of the monofunctional platinum(II) compounds but did not exhibit the longest distance from platinum atom to the edge of the non-labile ligand. Consequently, spatial orientation and/or hydrophobicity caused by the presence of a third aromatic ring may be significant factors in differentiating phenanthriplatin from the rest of its family. Derivatization of phenanthriplatin could further elucidate the structural components of this third aromatic ring that are responsible for causing NPM1 relocalization. We also note that the fast kinetics of DNA binding exhibited by phenanthriplatin may play a role in why phenanthriplatin is unique in the class of monofunctional platinum(II) compounds [6].

While oxaliplatin and phenanthriplatin both contain extended ligand structures around platinum(II), we find that steric properties alone are insufficient to explain the shared ability of these compounds to cause nucleolar stress. It is possible that monofunctional and bifunctional platinum(II) compounds may induce NPM1 relocalization through differential binding effects or mechanisms.

Acknowledgements This work was supported by the National Science Foundation [CHE1710721 to VJD], the NIH [T32 GM007759-29 to ECS] and used the Extreme Science and Engineering Discovery Environment (XSEDE), which is supported by National Science Foundation [ACI-1548562]. Computations were also performed on the PICS Coeus high performance computer, which is supported by the National

Science Foundation [1624776]. This work is also supported by the Department of Chemistry and Biochemistry, Department of Biology, Institute of Molecular Biology and the Material Science Institute at the University of Oregon.

Author contributions CEM: conceptualization, investigation, validation, writing original draft, visualization, and supervision. MVY: software, investigation, formal analysis, data curation, writing review and editing, and visualization. AMM: methodology, software, formal analysis, data curation, writing review and editing, and visualization. ECS: conceptualization, methodology, data curation, writing review and editing. MY: software, investigation, data curation, writing review and editing. CHH: project administration, funding acquisition, writing review and editing. VJD: project administration, funding acquisition, writing review and editing.

Data availability The datasets generated during and analyzed during the current study are available from the corresponding author on reasonable request.

References

1. Rosenberg B, Van Camp L, Krigas T (1965) Inhibition of cell division in escherichia coli by electrolysis products from a platinum electrode. Nature 205:698–699. https://doi.org/10.1038/205698a0
2. Kelland L (2007) The resurgence of platinum-based cancer chemotherapy. Nat Rev Cancer 7:nrc2167. https://doi.org/10.1038/nrc2167
3. Johnstone TC, Park GY, Lippard SJ (2014) Understanding and improving platinum anticancer drugs—phenanthriplatin. Anticancer Res 34:471–476
4. Sutton EC, McDevitt CE, Yglesias MV et al (2019) Tracking the cellular targets of platinum anticancer drugs: current tools and emergent methods. Inorg Chim Acta. https://doi.org/10.1016/j.ica.2019.118984
5. Park GY, Wilson JJ, Song Y, Lippard SJ (2012) Phenanthriplatin, a monofunctional DNA-binding platinum anticancer drug candidate with unusual potency and cellular activity profile. Proc Natl Acad Sci 109:11987–11992. https://doi.org/10.1073/pnas.1207670109
6. Almaqwashi AA, Zhou W, Naufer MN et al (2019) DNA intercalation facilitates efficient DNA-targeted covalent binding of phenanthriplatin. J Am Chem Soc 141:1537–1545. https://doi.org/10.1021/jacs.8b10252
7. Riddell IA, Agama K, Park GY et al (2016) Phenanthriplatin acts as a covalent poison of topoisomerase II cleavage complexes. ACS Chem Biol 11:2996–3001. https://doi.org/10.1021/acschembio.6b00565
8. Kellinger MW, Park GY, Chong J et al (2013) Effect of a monofunctional phenanthriplatin-DNA adduct on RNA polymerase II transcriptional fidelity and translesion synthesis. J Am Chem Soc 135:13054–13061. https://doi.org/10.1021/ja405475y
9. Gregory MT, Park GY, Johnstone TC et al (2014) Structural and mechanistic studies of polymerase η bypass of phenanthriplatin DNA damage. Proc Natl Acad Sci U S A 111:9133–9138. https://doi.org/10.1073/pnas.1405739111
10. Facchetti G, Rimoldi I (2019) Anticancer platinum(II) complexes bearing *N*-heterocycle rings. Bioorg Med Chem Lett 29:1257–1263. https://doi.org/10.1016/j.bmcl.2019.03.045
11. Bruno PM, Liu Y, Park GY et al (2017) A subset of platinum-containing chemotherapeutic agents kills cells by inducing ribosome biogenesis stress. Nat Med 23:461–471. https://doi.org/10.1038/nm.4291
12. Dhara SC (1970) A rapid method for the synthesis of *cis*-[Pt (NH3) 2Cl2]. Indian J Chem 8:193
13. Okada T, El-Mehasseb IM, Kodaka M et al (2001) Mononuclear platinum(II) complex with 2-phenylpyridine ligands showing high cytotoxicity against mouse sarcoma 180 cells acquiring high cisplatin resistance. J Med Chem 44:4661–4667. https://doi.org/10.1021/jm010203d
14. Bursac S, Brdovcak MC, Donati G, Volarevic S (2014) Activation of the tumor suppressor p53 upon impairment of ribosome biogenesis. Biochim Biophys Acta 1842:817–830. https://doi.org/10.1016/j.bbadis.2013.08.014
15. Nicolas E, Parisot P, Pinto-Monteiro C et al (2016) Involvement of human ribosomal proteins in nucleolar structure and p53-dependent nucleolar stress. Nat Commun 7:11390. https://doi.org/10.1038/ncomms11390
16. Schindelin J, Arganda-Carreras I, Frise E et al (2012) Fiji: an open-source platform for biological-image analysis. Nat Methods 9:676–682. https://doi.org/10.1038/nmeth.2019
17. Rueden CT, Schindelin J, Hiner MC et al (2017) Image J2: imageJ for the next generation of scientific image data. BMC Bioinform 18:529. https://doi.org/10.1186/s12859-017-1934-z
18. van der Walt S, Schönberger JL, Nunez-Iglesias J et al (2014) Scikit-image: image processing in Python. PeerJ 2:e453. https://doi.org/10.7717/peerj.453
19. Frisch M, Schlegel H, Scuseria G et al (2016) Gaussian09. Gaussian Inc., Wallingford
20. Perdew J, Burke K, Ernzerhof M (1996) Generalized gradient approximation made simple. Phys Rev Lett 77:3865–3868
21. Perdew J, Burke K, Ernzerhof M (1997) Errata: generalized gradient approximation made simple. Phys Rev Lett 78:1396
22. Pansini F, Neto A, de Campos M, de Aquino R (2017) Effects of all-electron basis sets and the scalar relativistic corrections in the structure and electronic properties of niobium clusters. J Phys Chem A 121:5728–5734
23. Marenich A, Cramer C, Truhlar D (2009) Universal solvation model based on solute electron density and a continuum model of the solvent defined by the bulk dielectric constant and atomic surface tensions. J Phys Chem B 113:6378–6396
24. Butler K, Hendon C, Walsh A (2014) Electronic chemical potentials of porous metal-organic frameworks. J Am Chem Soc 136:2703–2706
25. Blochl P (1994) Projector augmented-wave method. Phys Rev B 50:17953
26. Kresse G, Joubert D (1999) From ultrasoft pseudopotentials to the projector augmented-wave method. Phys Rev B 59:1758
27. Kresse G, Hafner J (1993) Ab initio molecular dynamics for liquid metals. Phys Rev B 47:558
28. Kresse G, Furthmuller J (1996) Efficient iterative schemes for ab initio total-energy calculations using a plane-wave basis set. Phys Rev B 54:11169
29. Kresse G, Hafner J (1994) Ab *initio* molecular-dynamics simulation of the liquid-metal–amorphous-semiconductor transition in germanium. Phys Rev B 49:14251–14269. https://doi.org/10.1103/PhysRevB.49.14251
30. Kresse G, Furthmüller J (1996) Efficiency of ab initio total energy calculations for metals and semiconductors using a plane-wave basis set. Comput Mater Sci 6:15–50. https://doi.org/10.1016/0927-0256(96)00008-0
31. Yang K, Wang M, Zhao Y et al (2016) A redox mechanism underlying nucleolar stress sensing by nucleophosmin. Nat Commun 7:13599. https://doi.org/10.1038/ncomms13599
32. Chen Y, Guo Z, Parsons S, Sadler PJ (1998) Stereospecific and kinetic control over the hydrolysis of a sterically hindered platinum picoline anticancer complex. Chem Eur J 4:672–676.

https://doi.org/10.1002/(SICI)1521-3765(19980416)4:4%3c672:AID-CHEM672%3e3.0.CO;2-8
33. Johnstone TC, Lippard SJ (2014) The chiral potential of phenanthriplatin and its influence on guanine binding. J Am Chem Soc 136:2126–2134. https://doi.org/10.1021/ja4125115

Affiliations

Christine E. McDevitt[1] · Matthew V. Yglesias[1,2] · Austin M. Mroz[1,3] · Emily C. Sutton[2,4] · Min Chieh Yang[1,3] · Christopher H. Hendon[1,3] · Victoria J. DeRose[1,2,3]

[1] Department of Chemistry and Biochemistry, 1253 University of Oregon, Eugene, OR 97403-1253, USA

[2] Institute of Molecular Biology, 1229 University of Oregon, Eugene, OR 97403, USA

[3] Materials Science Institute, 1252 University of Oregon, Eugene, OR 97403, USA

[4] Department of Biology, 1210 University of Oregon, Eugene, OR 97403, USA